Central European Journal of Energetic Materials
ISSN 1733-7178; e-ISSN 2353-1843

Cent. Eur. J. Energ. Mater. 2017, *14*(3): 573-588; DOI: 10.22211/cejem/75114

Detonation Reaction Characteristics for CL-20 and CL-20-based Aluminized Mixed Explosives

Danyang Liu, Lang Chen,* Chen Wang, Junying Wu

Beijing Institute of Technology,
5 South Zhongguancun Street, Haidian District, 100081 Beijing, China
**E-mail: chenlang@bit.edu.cn*

Abstract: The interfacial particle velocities for CL-20 and CL-20-based aluminized mixed explosives were measured by interferometry in order to analyze the aluminum reactions in the latter. The reaction characteristics were obtained, as well as a better understanding of the effects of aluminum powder on the detonation reaction zone length. Two functions were used to fit the particle velocity-time profiles, and their intersection was the corresponding Chapman-Jouget (CJ) point. From these profiles, the detonation reaction zone length and the aluminum reaction were then analyzed. CL-20-based explosives have a short reaction time (48 ns for a high CL-20 content), while the reaction time of CL-20/Al explosives increased with the aluminum content and particle size. Micron-scale aluminum particles barely reacted in the CL-20 detonation reaction zone, but instead reacted with the detonation products after the CJ point. This reduced the detonation pressure; however, the aluminum reaction can slow down the decrease in particle velocities. The start times of small-particle aluminum reactions were earlier than those of the larger particles. The 2-3-μm aluminum particles start to react within 1 μs after the CJ point, while the 200-nm particles may start to react in the reaction zone.

Keywords: detonation reaction zone, aluminum reaction, interfacial particle velocity, interferometry

1 Introduction

CL-20 explosives are very energetic with short reaction times and reaction zone lengths. The latter make it difficult to experimentally determine the detonation reaction characteristics. Currently, the interferometric measurement of particle velocities at the explosive/window interface is an effective way to investigate the

detonation wave structure and early detonation energy release. In this method, the interfacial particle velocity-time history is analyzed according to the Zeldovich-von Neumann-Doering (ZND) model, where the detonation reaction zone and the expansion zone of the products are separated by the Chapman-Jouget (CJ) point. Thus, the determination of the CJ point on the interfacial particle velocity-time profile is the key to revealing the detonation reaction characteristics.

Sheffield *et al*. [1] examined the detonation fronts of TNT-based and TATB-based explosives by using an ORVIS interferometer system, in order to measure the interfacial particle velocity history of the explosions against metal foil in contact with a water window. The foil thickness was 12 μm or 25 μm, however the shock reverberations in the foil made it difficult to directly estimate the location of the CJ point. To solve this problem, they took the intersection of the Hugoniots of the detonation products and the water as the CJ point *via* an impedance-matched solution. Seitz *et al*. [2] measured the interfacial particle velocity histories between TATB-based explosives and a transparent window (LiF, KBr, KCl and PMMA), using a Fabry-Perot interferometer system. A reflective aluminum film on the window was less than 1 μm, so the effects of the shock reverberation were negligible. This produced a clearer and more complete interfacial velocity profile. However, they observed that none of the detonation waves reached a steady state. Therefore, they estimated the steady-state reaction zone length by numerical calculations using the explicit hot-spot reaction-rate model and the HOM equation of state [3]. Han *et al*. [4] measured the interfacial particle velocity histories for PETN-based explosives and a PMMA window. They first calculated the detonation product isentrope with the VLW equation of state, and then calculated the CJ point velocity at the explosive/window by an impedance-matched solution. However, even with theoretical analyses, experiments are required to determine the calculation parameters. The accuracy of these parameters has a significant effect on the estimation of the detonation reaction length.

To directly determine experimentally the CJ point on the interfacial particle velocity-time profile, Fedorov *et al*. [5] measured the interfacial particle velocity histories of HMX-based explosives having various thicknesses. Depending on the assumption that the explosive particle velocity history in the reaction zone was constant in the steady detonation state, they determined the CJ point as the intersection of the multiple velocity-time profiles for the different thicknesses The disadvantage of this method is the large number of experiments required. Loboiko *et al*. [6] regarded the inflection on an interfacial velocity-time profile to be the CJ point. To reveal the inflection point, they plotted the time derivatives of the interfacial particle velocity profiles as two straight lines in semi-logarithmic

coordinates; the corresponding CJ point was the intersection of the two lines. In this way, they obtained the CJ point from just one interfacial particle velocity profile. However, the functional formulations to fit the derivative of the velocity-time profile had significant effects on the result.

Aluminum powder added to an explosive can increase the total energy of the explosive reaction, but it will also change the structure of the detonation reaction and the energy released. Lubyatinsky *et al*. [7] measured the aluminized RDX-based explosive/chloroform interfacial particle velocities. Their results indicated that an increase in aluminum particle diameter from 6 μm to 20 μm resulted in a small increase in the reaction zone length. To infer the early reaction rate of aluminum, Tao *et al*. [8] measured aluminized PETN- and TNT-based explosives/NaCl or LiF window interfacial particle velocities. The parameters of the ignition and growth reactive flow model were obtained from the results, and then the reaction rates of the aluminum with the detonation products were calculated. They found that 5-μm or 18-μm aluminum could react completely with the PETN detonation products within 1.5 μs after the CJ point.

Currently, the resolution of laser interferometry is 1-10 ns. Hence, for explosives with reaction times of less than 100 ns, such as CL-20 and HMX, this makes it difficult to analyze the structure of the detonation reaction. The behaviour of aluminum in explosions with short reaction times is an interesting research topic. In the present work, the detonation reaction characteristics of seven types of CL-20-based explosives containing different amounts and particle sizes of aluminum were experimentally investigated. Because of the short reaction times, an all-fiber "displacement interferometer system for any reflector" (DISAR) [9], with time resolution less than 5 ns, was employed to measure the explosive/window interfacial particle velocity. A new two-function fitting analysis was used to determine the CJ points on the interfacial velocity curves. The effects of the aluminum powder on the reaction zone length and its reaction in the CL-20-based explosives were then characterized.

2 Materials and Methods

A schematic diagram of the experimental apparatus for measuring the explosive/window interfacial particle velocity is shown in Figure 1. The CL-20-based explosive under test was initiated by a JO-9159 (HMX/FPM/95/5) 20-mm-diameter, 20-mm-thick cylindrical booster explosive. The booster was initiated by an electrical detonator and provided 36-GPa of pressure on the CL-20-based explosive. This input pressure led to a distance to detonation of less than 10 mm

for our experimental samples.

A 20-mm-diameter, 10-mm-thick LiF window was used as a transparent window for the DISAR laser interferometer used to measure the interfacial particle velocity. A 600-nm-thick aluminum film was vacuum-coated on one surface of the window to provide a reflective surface (middle of the film) for the laser light. The interferometer signal was converted into a particle velocity *vs.* time plot based on the Doppler-shift principle [10]. Because it was very thin, the velocity of the aluminum film can be assumed to be the same as that of the explosive/window interface. A digital storage oscilloscope in the DISAR was triggered by an electric probe sandwiched between the booster and the explosive. The time resolution of the measurement system was 1.5-5 ns.

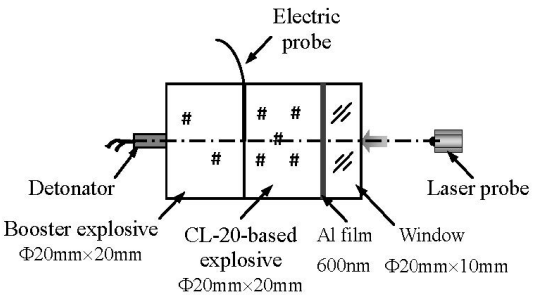

Figure 1. Schematic of the experimental arrangement

The experimental samples were C-1 explosives (CL-20/FPM/96/4), CL-20-based explosives containing various amounts and sizes of aluminum particles, and CL-20-based explosives containing LiF. The samples were pressed into 20-mm-diameter cylindrical charges with densities greater than 90% of the theoretical maxima. All of the aluminum particles were spherical.

3 Results and Discussion

3.1 Detonation reaction zone of C-1 explosive

Table 1 lists the C-1 explosive formulations and the experimental details. Figure 2 shows the interfacial particle velocity profiles obtained for the C-1 explosives with thicknesses of 20 mm and 30 mm. Each profile has an initial spike, followed by a rapidly decreasing detonation reaction zone and then a slowly declining detonation reaction products expansion (Taylor wave), as described by the ZND model. The spike had a rise time of 1.5 ns, which is the time resolution. The

absence of a distinct boundary point, corresponding to the CJ point, made it difficult to analyze the structure of the detonation wave directly. Therefore we used the direct experimental and impedance-match methods to estimate the CJ point on the profile, and then to develop a two-function fitting method.

Table 1. C-1 explosive formulations and experimental details

Formulation	Density [g/cm^3]	$\rho/\rho_{theoretical}$[a] [%]	Thickness of charge [mm]
CL-20/FPM/96/4	1.943	95.8	20
	1.916	94.5	20
	1.914	94.4	30

[a] $\rho/\rho_{theoretical}$ is the ratio between the explosive density (ρ) and the theoretical maximum density ($\rho_{theoretical}$).

Initially, Fedorov's direct experimental method [5] was used to determine the CJ point. In Figure 2, the two profiles gradually separate after a short period of overlap. The intersection of the profiles was determined to be the CJ point; from this it was estimated that the detonation reaction time t_{CJ} of the C-1 explosive was 47 ns.

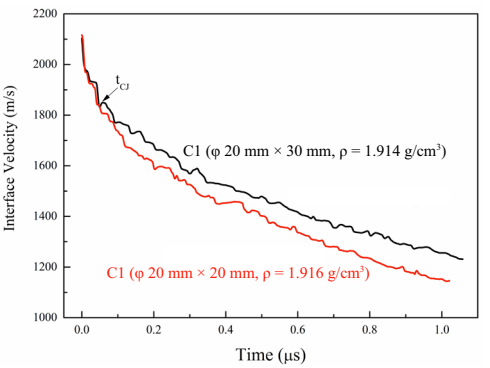

Figure 2. Interfacial velocity profiles for 20 mm and 30 mm-thick C-1 explosives

The Sheffield impedance-matching method [1] was then used to determine the position of the CJ point. Assuming consecutive velocity and pressure at the explosive/window interface, the wave propagation was solved in the pressure-particle velocity plane. Figure 3 shows the relevant Hugoniots and isentropes for the 1.916 g/cm^3 C-1 explosive and the LiF window.

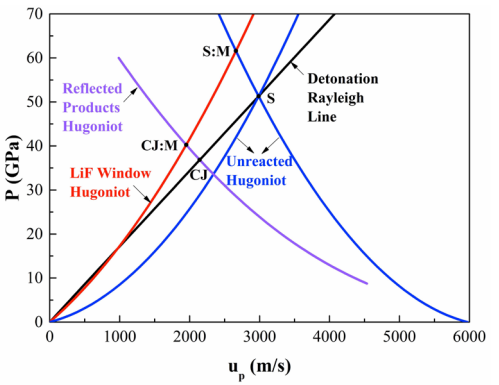

Figure 3. Hugoniots and isentropes for a 1.916 g/cm^3 C-1 explosive and the LiF window

The calculation details were as follows. The unreacted Hugoniot for C-1 is [11]:

$$U_S = 2.14 + 2.28u_p, \tag{1}$$

where U_s is the shock wave velocity and u_p is the particle velocity.

The Hugoniot for the detonation products was calculated by using the JWL equation of state, given by [12]:

$$P = A\left(1-\frac{\omega}{R_1V}\right)e^{-R_1V} + B\left(1-\frac{\omega}{R_2V}\right)e^{-R_2V} + \frac{\omega E}{V}, \tag{2}$$

where V is the relative volume; P is pressure and A, B, R_1, R_2, ω, and E are parameters.

The LiF shock Hugoniot was [13]:

$$U_S = 5.15 + 1.35u_p. \tag{3}$$

The spike (S point) was determined by the intersection of the detonation Rayleigh line and the unreacted Hugoniot, while the CJ point was the point of tangency of the detonation product Hugoniot and the detonation Rayleigh line. In Figure 3, the CJ point is at the intersection of the reflected product Hugoniot and the Rayleigh line. When the detonation shock wave spreads to the explosive/window interface, a reflected shock wave will then propagate in the explosive. The interface states then become S:M and CJ:M, respectively. The reaction

zone time can be then determined according to when the particle velocity goes below the CJ:M. From this analysis, the particle velocity was 1960 m/s, and thus it can be estimated that the reaction zone time of the C-1 explosive was 17 ns.

To accurately determine the CJ point on the interfacial particle velocity profile and to reduce the number of experiments required by the direct experimental method [5], a two-function fitting method was developed. It was used to fit the particle velocity-time curve and the CJ point was determined by the intersection on the curve.

In semi-logarithmic coordinates, the dependence of $-du_p/dt$ on t can be represented as a straight line before the CJ point [6]. So the interfacial particle velocity profile $u_p(t)$ was fitted by the exponential function for $t < t_{CJ}$:

$$u_p = u_3 \exp(-t / \tau) + u_4. \tag{4}$$

In the expansion zone of the detonation products after the CJ point, $u_p(t)$ was fitted by the polynomial function for $t > t_{CJ}$:

$$u_p = u_0 + u_1 t + u_2 t^2. \tag{5}$$

The u_0, u_1, u_2, u_3, u_4, and τ are fitting parameters and, at the point t_{CJ} Equations 4 and 5 have equal values. A fit to the experimental data for the 20-mm-thick, 1.916 g/cm^3 C-1 explosive is shown in Figure 4. The two functions provide a good fit to the velocity history. From the oscillation of the velocity history and the discontinuity of the experimental data, the CJ point was determined from the calculated intersection.

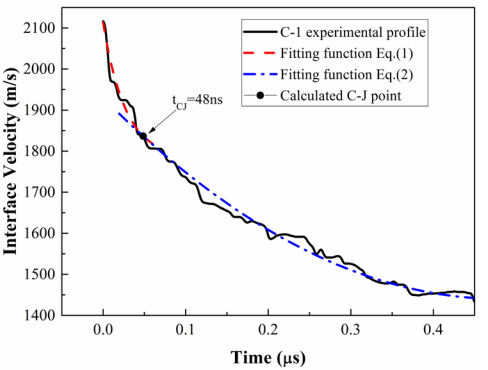

Figure 4. Functional fits to the experimental data for a 20 mm-thick, 1.916 g/cm^3 C-1 explosive

After locating the CJ point on the interfacial particle velocity profile and obtaining the time of the reaction zone, the reaction zone length and the CJ pressure could be calculated. According to the ZND model, the shock wave front and the reaction zone travel through the detonated explosive at detonation velocity D. Therefore, the reaction zone length x_0 is [14]:

$$x_0 = \int_0^{t_{CJ}} (D - u_p)\, dt. \tag{6}$$

From the LiF Hugoniot, the relationship between CJ pressure P_{CJ} and u_{pCJ} is [13]:

$$P_{CJ} = \frac{1}{2} u_{pCJ} [\rho_{m0}(5.15 + 1.35 u_p) + \rho_0 D], \tag{7}$$

where ρ_{m0} is the initial density of the LiF window (2.638 g/cm^3).

Table 2 lists the parameters of the C-1 explosive obtained by the three different methods described above. The electric probes were used to measure D. In Table 2, the parameters obtained by the two-function fitting are essentially the same as those obtained by the direct experimental method. Both CJ pressures are lower than that calculated by the impedance match method. This may be because of the much higher CJ pressure that was defined during the calibration of the JWL parameters. Moreover, lower initial densities result in longer reaction zone lengths.

Table 2. Parameters of the C-1 explosive obtained by the three different methods

Explosive	Density [g/cm^3]	D [m/s]	Two-function fitting method			Impedance-match method			Direct experimental method		
			t_{CJ} [ns]	x_0 [mm]	P_{CJ} [GPa]	t_{CJ} [ns]	x_0 [mm]	P_{CJ} [GPa]	t_{CJ} [ns]	x_0 [mm]	P_{CJ} [GPa]
C-1	1.943	9,100	38	0.27	34.7	14	0.10	38.1	-	-	-
	1.916	8,967	48	0.33	34.2	17	0.12	36.8	47	0.33	34.3

3.2 Detonation reaction zone of the aluminized CL-20-based explosive

Because the two-function fitting method can be used to determine the CJ point with just one profile, as indicated by the direct experimental method, it was used to process all of the experimental profiles. The parameters for the four kinds of CL-20-based explosives, containing 5 wt.% and 15 wt.% aluminum with diameters of 2-3 μm and 16-18 μm, are given in Table 3.

Table 3. Parameters for the CL-20/Al explosives with particle diameters of 2-3 μm and 16-18 μm

Formulation	Al diameter [μm]	Density [g/cm^3]	$\rho/\rho_{theoretical}$ [%]	Thickness of charge [mm]	t_{CJ} [ns]	D [m/s]	x_0 [mm]	P_{CJ} [GPa]
C-1/Al/95/5	2-3	1.940	94.3	20	48	8,895	0.35	30.14
	16-18	1.926	93.6	20	60	8,841	0.43	30.17
C-1/ Al/85/15	2-3	1.980	93.8	20	68	8,670	0.46	31.57
		1.979	93.8	30	73	8,667	0.48	31.20
	16-18	1.987	94.2	20	70	8,695	0.45	31.47
		1.987	94.2	40	67	8,695	0.45	31.64

When the amount of aluminum was 5 wt.%, the reaction time of the CL-20/Al explosive with 2-3-μm aluminum was the same as that of C-1. An increase in aluminum particle diameter from 2 μm to 18 μm resulted in a reaction time increase from 48 ns to 60 ns and an increase in zone length from 0.35 mm to 0.43 mm. However, when the amount of aluminum was 15 wt.%, the reaction time of the two compositions were similar (70 ns). This means that an increase in the aluminum content reduces the effect of the aluminum particle diameter on the reaction zone. Furthermore, the CJ pressures for the CL-20/Al explosives are all approximately 31 GPa, less than that for C-1. The thickness of the experimental charge had no appreciable effect on the reaction time, so the explosives reached a stable state.

To make the effect of the aluminum particle diameter on the explosives with 15 wt.% aluminum clearer, more compositions were tested and their parameters are given in Table 4.

Table 4. Parameters for CL-20/Al explosives loaded with 15 wt.% aluminum

Formulation	Al diameter	Density [g/cm^3]	$\rho/\rho_{theoretical}$ [%]	Thickness of charge [mm]	t_{CJ} [ns]	D [m/s]	x_0 [mm]	P_{CJ} [GPa]
C-1/Al/85/15	200 nm	1.935	91.7	20	92	8,510	0.62	25.88
	40-50 μm	2.006	95.1	40	99	8,764	0.68	31.64

From Table 4, as the aluminum particle diameter was increased to 40-50 μm, the reaction time increased to 99 ns, which is more than twice that of the aluminum-free C-1. This means that the larger the aluminum particles, the longer the reaction time. However, t_{CJ} was unexpectedly 92 ns for the CL-20/Al explosive filled with 200-nm particles. A discussion of the CL-20/Al explosive filled with 200-nm particles is included in Section 3.3 below.

The effects of the aluminum particles on the reaction zone derive from two main sources. Firstly, the dynamics between the aluminum particles and the explosive could affect the structure of the detonation wave because of the higher aluminum impedance [15]. We found the reaction time of a CL-20-based explosive loaded with 15 wt.% LiF (1.953 g/cm^3, 20 mm thickness) was 57 ns, longer than that of C-1, using the method described in Section 2. Thus, the addition of inert materials can also increase the detonation reaction time. Secondly, if the aluminum particles start to react in the detonation reaction zone, the reaction energy may increase the release time of the explosive detonation energy, which increases the reaction time. However, most previous reports have indicated that the aluminum primarily reacts with the detonation products after the detonation wave front [16, 17]. Hence, to understand the effects on the reaction zone and the aluminum reaction, particle velocities during the detonation product expansion should be analyzed.

3.3 Analysis of the aluminum reaction

The effects of the aluminum reaction on the velocity of the detonation products after the CJ point were analyzed. For this analysis, all of the charges had a thickness of 20 mm. Figure 5 plots the interfacial particle velocity profiles for the C-1 explosives and CL-20/Al explosives loaded with 5 wt.% of 2-3-μm or 16-18-μm aluminum. The black dots are time positions of the CJ points.

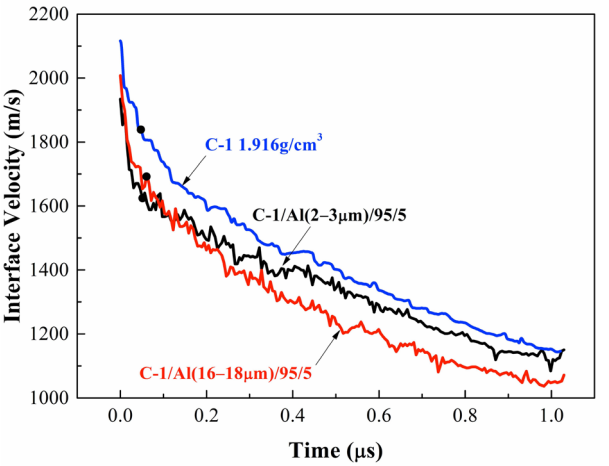

Figure 5. Interfacial particle velocity *vs.* time for the C-1 explosives and CL-20/Al explosives loaded with 5 wt.% of 2-3-μm or 16-18-μm aluminum

In Figure 5, the two aluminized explosives have higher densities and lower velocity in the reaction zone than the C-1 explosive. This indicates a low reactivity for the aluminum in the reaction zone. After the detonation reaction, the velocity of the CL-20/Al explosive with 16-18-μm aluminum decreased at the same constant rate as the C-1 explosive. However, for the CL-20/Al explosive with 2-3-μm aluminum, there was a second stage where the velocity did not decrease as fast. This stage appears 0.1 μs after the CJ point. This is because the 2-3-μm aluminum mainly reacted with the detonation products at 0.1 μs, and the energy released counteracted the decreasing particle velocity. By contrast, without this extra energy, the detonation products of the CL-20/Al explosive loaded with 16-18-μm aluminum expanded because of the rarefaction wave.

Figure 6 plots the velocity profiles for CL-20/Al explosives loaded with 15 wt.% of 200-nm or 2-3-μm aluminum and CL-20/LiF explosive loaded with 15 wt.% of LiF (1.953 g/cm^3). The dots are time positions of the CJ points. In Figure 6, LiF was used to replace aluminum. LiF is inert in explosives and has similar physical properties to aluminum; thus, it is expected to behave as 'inert aluminum' [18].

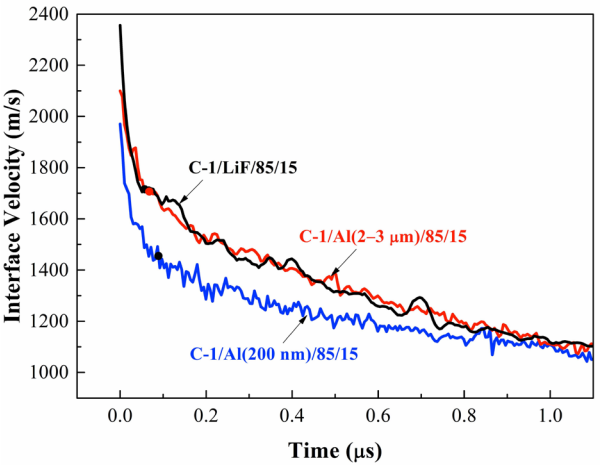

Figure 6. Interfacial particle velocity *vs.* time for CL-20/Al explosive loaded with 15 wt.% of 200-nm or 2-3-μm aluminum and CL-20/LiF explosive loaded with 15 wt.% of LiF

In Figure 6, the wave profiles for the CL-20/Al explosive loaded with 15 wt.% of 2-3-μm aluminum almost coincides with that of the CL-20/LiF explosive loaded with 15 wt.% LiF. Therefore, we can conclude that, like LiF, the 15 wt.% of 2-3-μm aluminum was inert during the 1-μs test times. Conversely, the decreasing rate of velocity for the CL-20/Al explosives loaded with 15 wt.% 200-nm aluminum was significantly slower than that of the two other explosives. The second stage appeared almost at the same time as the CJ point.

We estimated from Figures 5 and 6 that the aluminum reaction starts earlier for smaller particles and lower content. The 200-nm aluminum, being the smallest size, started to react earliest, as expected. The start time of the reaction was almost at the CJ point. Moreover, the reaction time for the CL-20/Al explosive loaded with 200-nm aluminum was unexpectedly large. This indicates that 200-nm aluminum may start to react in the detonation reaction zone. However, because of the much lower interfacial particle velocity in the reaction zone, the energy released by the aluminum may not support propagation of the detonation wave.

To understand the effects of the aluminum on the energy release in the reaction zone, the energy release efficiency per unit volume and time in the reaction zone (η) was defined as:

$$\eta = Q\omega\rho_0 / t_{CJ}, \tag{8}$$

where Q is the energy released by energetic materials per unit mass and ω is the amount of energetic material in the mixed explosive. A larger η gives a larger energy released per unit time in the detonation reaction zone. For CL-20-based explosives with micron-diameter aluminum particles, CL-20 is the only energetic material, so Q is the explosion heat of CL-20, 6234 J/g [19]. The energy release efficiency in the reaction zone (η) of CL-20/Al explosives with micron-diameter aluminum particles is shown in Figure 7.

In Figure 7, the C-1 explosive has the highest η and the increase in aluminum content results in a lower energy release efficiency in the reaction zone. When the diameter of the aluminum particles was 2-18-μm, the increase in the diameter of the aluminum significantly decreased the η of the explosives with 5 wt.% aluminum, but had almost no influence on the η of explosives with 15 wt.% aluminum.

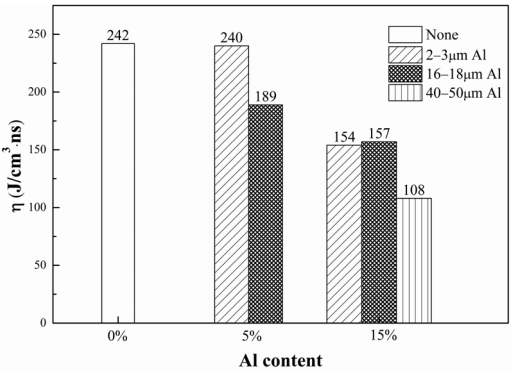

Figure 7. Energy release efficiency in the reaction zone *vs*. aluminum content for CL-20/Al explosives

After the CJ point, the ratio (u_{t1}/u_{CJ}) of the interfacial particle velocity at 1 μs after the spike (u_{t1}) to the interfacial particle velocity at the CJ point (u_{CJ}) is perceived as a decreasing range of the detonation product velocities. Figure 8 shows the u_{t1}/u_{CJ} of CL-20/Al explosives with a charge thickness of 20 mm.

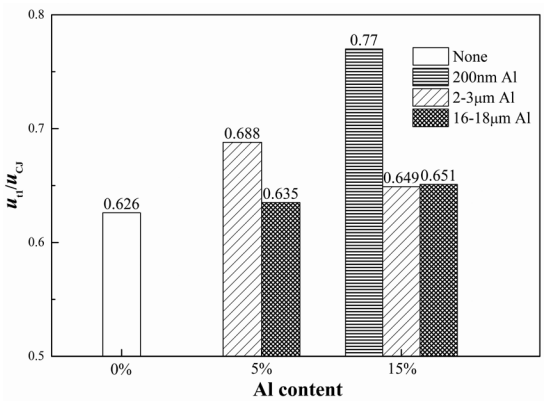

Figure 8. u_{t1}/u_{CJ} *vs*. aluminum content for CL-20/Al explosives of thickness 20 mm

In Figure 8, the u_{t1}/u_{CJ} of C-1 explosive is lower than those of the aluminized explosives. When the aluminum particles exhibit inert behaviour, the u_{t1}/u_{CJ} of a CL-20/Al explosive is close to 0.65. However, when the aluminum powder begins to react, the u_{t1}/u_{CJ} of the explosive will increase significantly. This indicates that the aluminum reaction leads to a longer trajectory of the detonation products at a relatively high velocity, and thus a stronger capability.

4 Conclusions

Seven types of CL-20-based aluminized explosives with 0%, 5%, and 15% aluminum content and particle diameters of 200 nm, 2-3 μm, 16-18 μm and 40-50 μm were investigated by measurement of the particle velocities at the explosive/window interface. The reaction characteristics of the explosives were obtained and provided a better understanding of the effects of aluminum powder on the detonation reaction in these explosives. A two-function fitting method was developed to determine the corresponding CJ positions in the velocity profiles.

The main conclusions were as follows:

(1) The reaction time for C-1 explosives varies over 38-48 ns, when its density varies over 1.916-1.943 g/cm^3. The addition of aluminum powder to the CL-20 explosives increases the reaction zone length. When the aluminum particles were micron sized, the zone lengths increased with the amount of aluminum and the particle size.

(2) Micron-diameter aluminum particles did not react in the CL-20 explosive

reaction zone and reacted mainly with the detonation products. Smaller particle diameters and/or lower aluminum contents in the CL-20 resulted in earlier start times of the aluminum reaction. 200-nm particles may react in the CL-20 explosive reaction zone. However, the energy released by the aluminum reaction does not support the detonation wave.

(3) The inert behaviour of aluminum powder in the CL-20 explosive reaction zone decreases the energy release efficiency in the reaction zone. The reaction between the aluminum powder and the detonation products counteracts the decrease in explosive particle velocity of the products.

Acknowledgments

The authors wish to thank Lian-Sheng Zhang for his assistance in operating the interferometer. Discussions with Wen-Bin Huang were helpful in experimentally understanding the structures of the detonation waves. The test samples and the testing ground were provided by Gansu Yinguang Chemical Industry Group Co., Ltd.

References

[1] Sheffield, S. A.; Bloomquist, D. D.; Tarver, C. M. Subnanosecond Measurements of Detonation Fronts in Solid High Explosives. *J. Chem. Phys.* **1984**, *80*(8): 3831-3844.

[2] Seitz, W.; Stacy, H.; Wackerle, J. Detonation Reaction Zone Studies on TATB Explosives. *8th Int. Symp. Detonation*. Albuquerque, USA **1985**, 123-132.

[3] Seitz, W.; Stacy, H.; Engelke, R.; Tang, P.; Wackerle, J. Detonation Reaction-zone Structure of PBX9502. *9th Int. Symp. Detonation*, Portland, USA **1989**, 657-669.

[4] Han, Y.; Long, X. P.; Liu, L. Experimental Study on Explosive Reaction Zone. (in Chinese) *1st Symposium on Hazardous Materials and Security Emergency Technology*. Chongqing, China **2011**, 230-235.

[5] Fedorov, A.; Menshikh, A.; Yagodin, N. On Detonation Wave Front Structure of Condensed High Explosives. *10th American Physical Society Topical Conference on Shock Compression of Condensed Matter*, Amherst, USA **1998**, 735-738.

[6] Loboiko, B.; Lubyatinsky, S. Reaction Zones of Detonating Solid Explosives. *Combust., Explos. Shock Waves (Engl. Transl.)* **2000**, *36*: 716-733.

[7] Lubyatinsky, S.; Loboiko, B. Reaction Zone Measurements in Detonating Aluminized Explosives. *Conference of the American Physical Society Topical Group on Shock Compression of Condensed Matter*, Seattle, USA **1996**, 779-782.

[8] Tao, W. C.; Tarver, C. M.; Kury, J. W.; Lee, C. G.; Ornellas, D. L. Reactive Flow Modeling of Aluminum Reaction Kinetics in PETN and TNT Using Normalized Product Equation of State. *10th Int. Symp. Detonation*, Boston, USA **1993**, 628-636.

[9] Weng, J. D.; Tan, H.; Wang, X.; Ma, Y.; Hu, S.; Wang, X. Optical-fiber Interferometer for Velocity Measurements with Picoseconds Resolution. (in Chinese) *Appl. Phys. Lett.* **2006**, *89*: 111101.
[10] Wang, D. T.; Li, Z. R.; Wu, J. R.; Liu, S. X.; Liu, J.; Meng, J. H.; Liu, Q. An Optical-fiber Displacement Interferometer for Measuring Velocities of Explosively-driven Metal Plates. (in Chinese) *Explos. Shock Waves* **2009**, *29*: 105-108.
[11] Chen, L.; Pi, Z. D.; Liu, D. Y.; Yang, K.; Wu, J. Y. Shock Initiation of the CL-20 Based Explosive C-1 Measured with Embedded Electromagnetic Particle Velocity Gauges. *Propellants Explos. Pyrotech.* **2016**, *41*(6): 1060-1069.
[12] Liu, D. Y.; Chen, L.; Yang, K.; Zhang, L. S. Study of the Method of Parameters Calibration of Detonation Products JWL Equation of State for CL-20-based Explosives. (in Chinese) *Acta Armamentarii* **2016**, *37* (Suppl. 1), 141-145.
[13] Chen, Q. C.; Jiang, X. H.; Li, M.; Lu, X. J.; Peng, Q. X. Ignition and Growth Reactive Flow Model for HNS-IV Explosive. (in Chinese) *Explos. Shock Waves* **2012**, *32*: 328-332.
[14] Lubyatinsky, S.; Loboiko, B. Density Effect on Detonation Reaction Zone Length in Solid Explosives. *10th American Physical Society Topical Conference on Shock Compression of Condensed Matter*, Amherst, USA **1998**, 743-746.
[15] Wang, C.; Chen, L.; Lu, J. Y. Study on Reaction Process of Small-sized Aluminum Particle in Detonation Reaction Products. (in Chinese) *Acta Armamentarii* **2012**, *33* (Suppl. 2): 30-36.
[16] Cook, M. A.; Filler, A. S.; Keyes, R. T.; Partridge, W. S.; Ursenbach, W. Aluminized Explosives. *J. Phys. Chem.* **1957**, *61*: 189-196.
[17] Chen, L.; Zhang, S. Q.; Zhao, Y. H. Study of the Metal Acceleration Capacities of Aluminized Explosives with Spherical Aluminum Particles of Different Diameter. (in Chinese) *Explosion and Shock Waves* **1999**, *19*: 250-255.
[18] Bjarnholt, G. Effects of Aluminum and Lithium Fluoride Admixtures on Metal Acceleration Ability of Comp B. *6th Int. Symp. Detonation*. Coronado, USA **1976**, 510-521.
[19] Simpson, R. L.; Urtiew, P. A.; Ornellas, D. L.; Moody, G. L.; Scribner, K. J.; Hoffman, D. M. CL-20 Performance Exceeds that of HMX and Its Sensitivity Is Moderate. *Propellants Explos. Pyrotech.* **1997**, *22*: 249-255.